Eleventh International Conference on CFD in the Minerals and Process Industries
CSIRO, Melbourne, Australia
7-9 December 2015

APPLICATION OF A DISCRETE PHASE MODELLING APPROACH TO INDUSTRIAL SCALE FLOWS

Allan LOVE[1*]

[1] Doosan Boiler R&D Centre, Renfrew, Renfrewshire, UK
*Corresponding author, E-mail address: allan.love@doosan.com

ABSTRACT

Increasing environmental awareness and legislation is driving the continuous improvement in efficiency and emissions performance of pulverised fuel power plants. Doosan Babcock use Computational Fluid Dynamics as both a design and troubleshooting tool to improve the operation, upgrade and design of thermal plant components to meet this aim. This paper presents the results of a validation and uncertainty quantification exercise for a gas-particle modelling approach. The gas-particle flow model is based on the Eulerian-Lagrangian approach in the commercial CFD code ANSYS Fluent with additional particle model physics added with User Defined Functions. The flow of a coal equivalent particulate through a pipe run and annular coal burner is investigated. The CFD results are quantitatively compared with the experimental pressure drop and outlet mass distribution. A qualitative comparison of the CFD results and experimental and plant erosion patterns also showed good agreement. Examples of how this detailed CFD analysis can directly benefit our design of experiments, processes and ultimately our customers are also discussed.

NOMENCLATURE

C_R	constant for particle rotation
e	coefficient of restitution
F_D	acceleration due to drag [ms^{-2}]
g	acceleration due to gravity [ms^{-2}]
I	moment of inertia [$kg\ m^2$]
k	turbulent kinetic energy [$J\ kg^{-1}$]
p	pressure [Pa]
S	source term
T	torque [Nm]
t	time [s]
u	velocity [ms^{-1}]
Re_r	particle Reynolds number for rotation

Greek Symbols

α	impact angle [˚]
ε	turbulent energy dissipation rate [m^2s^{-3}]
ξ	normally distributed random number
ω	angular velocity [rad s^{-1}]
Ω	relative angular velocity [rad s^{-1}]
ρ	density [$kg\ m^{-3}$]
τ	stress tensor [Pa]
μ	coefficient of friction
γ	standard deviation of wall roughness angle [˚]

Subscripts

0	impact angle of 0˚
c	continuous phase
dpm	discrete phase model
p	particle/discrete phase
e	impact angle for coefficient of restitution
μ	impact angle for coefficient of friction

INTRODUCTION

For pulverised fuel power plants pneumatic conveying is used to transfer the solid particles from the mill to the burner through an often complex piping system. Increasing environmental awareness and legislation is driving the continuous improvement in efficiency and emissions performance of pulverised fuel power plants. Doosan Babcock use CFD as both a design and troubleshooting tool to inform the operation, upgrade and design of pulverised fuel systems. The main quantities of interest include system pressure drop, particle distributions and erosion rates. With confidence in the prediction of such quantities with CFD, the application of CFD can be extended to inform increasingly detailed design.

For gas-particle flows, pneumatic conveying studies are conducted at relatively small scale compared to thermal plant, for example in narrow pipe diameters and for simple geometries (Tsuji and Morikawa (1982), Giddings et al. (2004), Laín and Sommerfeld (2013)). This has facilitated the use of detailed measurement techniques, such as Laser Doppler Anemometry, and the development and validation of particle force models. However, the effects of geometry scale have been shown to be significant in fluidised beds where particle clustering effectively lowers the particle drag coefficient (Li and Kwauk (1994)). Where the volume fraction of the discrete phase is not accounted for in the continuous phase continuity and momentum equations and/or coarse grids are utilised the effect of particle clustering is not resolved adequately. Sub-grid scale models can be utilised in these cases (Schneiderbauer et al. (2013) and Love et al. (2015)). For dilute pneumatic conveying systems regions of high particle concentration occur as the particle ropes or at the onset of saltation. Therefore, it is pertinent to investigate gas-particle flow models for application to pneumatic conveying flows across a range of scales.

This paper will compare a gas-particle modelling approach with a full scale experiment to evaluate the level of confidence in the modelling approach. The experiment is a study of the flow of a coal equivalent solid, pumice stone, through a pipe run and coal burner geometry. The uncertainty in the measured quantities has been estimated and used to inform the uncertainty in the model result. The CFD modelling approach utilises the commercial CFD software ANSYS Fluent 15.0.7 with additional particle model physics included through User Defined Functions (UDF). Additional particle models include

injection, particle wall collisions accounting for wall roughness effects, particle rotation, torque and erosion.

EXPERIMENT DESCRIPTION

The pipe and burner geometries are shown in Figure 1 and Figure 2. The operating conditions are summarised in Table 1. The system is under vacuum, with a steady feed of pumice supplied via a screw feeder just downstream of the inlet, the burner outlet was divided into an internal circular outlet and 8 annular sectors as shown in Figure 8. Here the air mass flowrate through the 9 outlets was balanced to ensure an equal area weighted average velocity at each outlet. Burner pressure drop, average outlet mass distribution and erosion pattern results were obtained.

EXPERIMENTAL UNCERTAINTY ANALYSIS

Results for industrial scale flows are an important part of validating CFD models. To determine the most significant factors influencing the robustness of the validation data an uncertainty analysis has been performed. Where available the reported errors in the measured quantities have been used to obtain the relative uncertainty within a 95% confidence interval for the inputs to the CFD analysis (air and solid mass flowrates and pressure drops). These are summarised in Table 2. Measurement errors, for example in velocity and pipe diameter, were combined using the procedures described by the British Standards Institution (2005).

Significant uncertainties were found for the air and pumice mass flow rates. The air and pumice flow rates are first calibrated based on the measurement of velocity and pipe diameter. However, for each test a set point approach was used with a significant reading error. The uncertainty in the outlet distribution was hindered by the geometry tolerance at the measurement section. For two phase flow the uncertainty in the burner pressure drop fluctuates due to a slight unsteadiness in the feed. Improvements to the measurement procedures have been identified which should reduce the uncertainty in future tests.

CFD MODEL DESCRIPTION

Steady state, isothermal simulations were performed using commercial CFD package ANSYS Fluent R15.0.7, which solves the Navier Stokes equations using the finite volume method. The continuity and momentum equations for the continuous phase are:

$$\nabla.(\rho\,\overrightarrow{u_c}) = S_{dpm} \tag{1}$$

$$\nabla.(\rho\overrightarrow{u_c}\overrightarrow{u_c}) = -\nabla p + \nabla\tau + \rho\vec{g} + S_{dpm} \tag{2}$$

where S_{dpm} is the source term due to the discrete phase. Turbulence was modelled using the Realizable k-ε model.

The pressure based solver and SIMPLE algorithm were used for pressure correction. Discretisation using PRESTO! for pressure, third order MUSCL for momentum and second order upwind schemes for turbulent kinetic energy and dissipation. The single phase flow cases were initially solved to the limit for single precision and subsequently the two-phase flow was simulated. Multiple monitors for pressure, velocity and particle concentration were used to judge convergence of the two phase flow. The boundary conditions for each model are summarised in Table 3.

Discrete Phase Model

The particle properties for each phase are also shown in Table 3. The discrete phase was modelled using the Lagrangian approach with Fluent's Discrete Particle Model (DPM). Here the Lagrangian tracking method is used to solve the individual theoretical particle trajectories by equating their inertia with external forces:

$$\frac{du_p}{dt} = \overrightarrow{F_D} + \frac{\vec{g}(\rho_p - \rho_c)}{\rho_p} + \overrightarrow{F_{other}} \tag{3}$$

$$I_p \frac{d\overrightarrow{\omega_p}}{dt} = \vec{T} \tag{4}$$

Additional particle boundary conditions and forces were included through the User Defined Function interface.

The particles are injected at an inlet surface representing the silo inlet with a velocity vector determine from the mean and standard deviation of the components in Table 3. The non-spherical drag model of Haider and Levenspiel (1989) with shape factor of 0.7 was used for the pumice particles.

Particle-wall interaction was modelled using the wall collision and stochastic wall roughness model of Sommerfeld (1999), with wall collision model parameters based on the reported quartz particles values (pumice stone being 75% quartz). The restitution and friction coefficients were dependent on the wall impact angle as follows:

$$e = MAX\left(1 + \frac{1 - e_h}{0 - \alpha_e}\alpha, e_h\right) \tag{5}$$

$$\mu = MAX\left(\mu_0 + \frac{\mu_0 - \mu_h}{0 - \alpha_\mu}\alpha, \mu_h\right) \tag{6}$$

The collision of a particle with a wall results in particle rotation and the angular momentum of the particle is dissipated by applying the effect of torque from the continuous phase. This was modelled according to the approach described by Laín and Sommerfeld (2008):

$$\vec{T} = \frac{\rho}{2}\left(\frac{d_p}{2}\right)^5 C_R|\vec{\Omega}|\vec{\Omega} \tag{7}$$

where

$$\vec{\Omega} = \overrightarrow{\omega_c} - \overrightarrow{\omega_p} \tag{8}$$

$$C_R = \frac{64\pi}{Re_r} \qquad Re_r \le 32 \tag{9}$$

or using the extension to higher particle Reynolds numbers defined by Denis et al. (1980)

$$C_R = \frac{12.9}{Re_r^{0.5}} + \frac{128.4}{Re_r} \qquad 32 < Re_r < 1000 \tag{10}$$

and

$$Re_r = \frac{\rho_c d_p^2 |\overrightarrow{\omega_d}|}{\mu} \tag{11}$$

Particle collisions have been neglected in this initial study. Although the maximum mean volume fractions are <0.001m^3/m^3 and the effects of particle-particle interaction and solids volume fraction could be considered negligible, local particle concentration effects play a role on the overall behaviour in both simple and complex geometries and future work will investigate a particle collision model in Fluent's steady state solver.

Particle-turbulence interaction was modelled using Fluent's Discrete Random Walk model where the particle sees an instantaneous velocity component according to:

$$u_{c,i}^{'} = \xi_i \sqrt{\frac{3k}{2}} \quad (12)$$

where the lifetime of an eddy is defined as 0.3k/ε. As this model is isotropic it has potential short comings for confined flows as in reality the velocity fluctuation in the wall normal direction is dampened close to the wall. However, it will be shown that the initial results are promising for this study.

An indication of erosion propensity is determined over the duration of the burner experiment using a water based paint coating. The erosion rate was modelled using a normalized erosion rate for a ductile material as follows:

$$ER = \dot{m}.f(\alpha).V^{2.5} \quad (13)$$

Where V>5m/s and f(α) is shown in Figure 3.

CFD Cases

The CFD cases investigated are shown in Table 4. The sensitivity of the pressure drop to the mesh size and number of particle tracks has been determined. Additional sensitivities have been performed for the drag and wall collision model parameters.

The standard mesh (2.2m, cells) was refined to (12.8m cells) and the difference between the single phase pressure drop was within 0.5%. Figure 5 shows the results of the particle track independence study. The highest value of 4 equally distributed monitor points at the outlet is shown for particle concentration. The number of DPM iterations to convergence and final values are consistent between both cases and so 50,000 tracks are sufficient. Figure 5 shows a cycling of the particle concentration which will affect the outlet distribution and an average over 20 DPM iterations was deemed sufficient as shown in

Figure **4**. The CFD results were therefore judged to be independent of the mesh and number of tracked particles.

RESULTS

Figure 6 shows normalised burner pressure drop results compared with the experimental data and a sensitivity of the model parameters. It can be seen that the base CFD model predicts the single phase burner pressure drop at 98% of the experimental pressure drop. But the model over predicts by 24% for the two phase flow. In the case of the burner with internals (case 7 and 8), the single phase flow is over predicted by 6% and the two phase flow by 33%, although the results lie within the experimental error when accounting for the uncertainty in CFD flowrates.

Computing the pressure drop based on the static pressure values close to the experimental pressure tapping locations resulted in an improved pressure drop prediction by 5-12% in all cases compared to simply taking an area weighted average value for a cross-section in the computational domain. Therefore, it is important to clearly identity the measurement locations.

The sensitivity of the model to the wall collisions and drag parameters was investigated in cases 5 and 6. It was expected that lowering the drag coefficient and approaching elastic collisions at the wall would reduce the pressure drop. Indeed the burner pressure drop fell in both cases but not significantly. Given this sensitivity analysis it is concluded that the over prediction of the burner pressure drop is possibly due to the uncertainty in the experimental flowrates. The re-acceleration of the particles following a reduction in velocity at the bend is likely to be the most significant contributor to the pressure drop. The pressure drop is particularly sensitive to the flowrate values due to being proportional to the square of the air velocity and directly proportional to the solid mass flowrate. Therefore, uncertainties in these quantities will directly show up in the pressure drop measurement.

However, the absence of additional model physics could also account for some of the difference. The absence of inter-particle collisions within the CFD model was shown to reduce the number of wall collisions and thus pressure drop by Oesterlé and Jean (1993) and thus could also have an impact. In addition, the effects of particle clustering/roping allow particles to shelter behind each other effectively lowering the drag force on each individual particle and thus could delay the re-acceleration of the particles within the burner. This would manifest as a lower pressure drop immediately following a pipe bend.

Figure 7 illustrates the main path of the particles within the geometry. A region of higher particle volume fraction forms within the geometry due to the first bend, the particles them begin to spiral as a result of the second bend ultimately being mal-distributed at the entrance to the burner. Figure 8 shows the resulting burner outlet distribution for both cases 3 and 5. It can be seen that the particle wall collision model parameters (case 3) have a significant, positive impact on the outlet distribution. The uncertainty in the outlet distribution was estimated at 33% and the mean and maximum difference between the CFD outlet distribution in case 3 and the experiment were 20% and 60%, respectively. The uncertainty estimate is based only on the calibration of the air flow distribution and the effect of different solids flowrates through each outlet pipe on the uniformity of the outlet flow was not quantified. The agreement between the CFD and experimental distribution is good however. This may be improved with the inclusion of additional particle model physics or equally improvements to the experimental measurement. Note that the experimental results showed that the outlet distribution was not as sensitive to changes in the air flowrate, compared to the burner pressure drop.

Having demonstrated good agreement with the experimental results for the simple case of a burner with no internals the modelling approach was applied to a burner with internals (Case 7, 8). This geometry is illustrated in Figure 2. Figure 9 shows the experimental erosion pattern, plant erosion pattern and the predicted

CFD erosion pattern for this geometry. Qualitative agreement is obtained between the plant, experimental and CFD results on both the inner and outer pipe surfaces. This demonstrates that not only the outlet distribution but distribution within the geometry is in good agreement and gives confidence in determining the erosion regions in other similar geometries.

DISCUSION AND CONCLUSION

This paper reports on a pneumatic conveying study relevant to full scale pulverised fuel plant. Experimental results for a full scale coal burner geometry were compared with a CFD model for gas-particle flows. The uncertainties in the experimental measurements which are significant to the CFD analysis have been estimated. Only the main model input parameters of air and solids mass flowrates and their impact on pressure drop have been considered. Additional uncertainty remains regarding the definition of the particle size distribution and particle shape. Identifying the uncertainty in the measurement quantities will allow improved design of experiments and procedures in the future.

Good agreement was obtained between the single phase pressure drops within the two burner geometries considered. For the two-phase flow the burner pressure drop appeared consistently over predicted in each case but lay within the experimental error. Good agreement was also obtained with the burner outlet distribution with a mean and maximum deviation from the experimental values of 20% and 60% respectively. Finally, qualitative agreement was observed for the CFD erosion prediction against the experiment and plant test cases.

A mesh of 2,200,000 cells and 50,000 particle tracks were determined to be sufficient. Potentially improved agreement with the experimental data could be achieved through additional particle force models, such as inter-particle collisions, particle shape, lift forces and structure dependent drag formulations. Without quantifying the effect of these models at this scale questions will remain on using the model to extrapolate far from the experimental results reported here.

This analysis has been used to help define our confidence in the two-phase flow modelling approach to help aid experimental design, CFD model development and ultimately plant design and modification. Overall the application of additional models for gas-particle flows has resulted in good agreement with the particle flow in a complex geometry.

Case	**Burner**
Air Flowrate [kg/s]	3.718
Solids Flowrate [kg/s]	1.725
Solids Loading [kg/kg]	0.46
Scale (Diameter)[m]	0.457
Temperature [K]	293
Pressure [Pa]	101315
Pipe Material	Plastic
Particles	Pumice
Mass Mean Particle Diameter [µm]	57
Density [kg/m^3]	2300

Table 1: Experimental case set up.

	Single Phase	**Two Phase**
Uncertainty	**Relative standard expanded uncertainty [%]**	**Relative standard expanded uncertainty [%]**
Air Flowrate [kg/s]	19.5	19.5
Solid Flowrate [kg/s]	NA	13.7
Outlet Distribution [kg]	34	34
Pressure Drop Measured [Pa]	1.4	10
CFD Burner Pressure Drop [Pa]	34.9	38.77

Table 2: Estimated uncertainty for CFD inputs.

Case	**Burner**
Particle Injection Velocity [m/s]	(0, -2.1, 0)
Standard deviation in injection velocity [m/s]	(0.1, 0.1, 0.1)
Particle Size Distribution [µm]	22 to 177
Wall Collision Parameters e_h μ μ_0 α_e α_μ γ	 0.55 0.8 0.15 27˚ 50˚ 2.6˚
Drag Model Shape Factor	0.7
Air Inlet	Velocity profile, 4% turbulence intensity
Air wall	No slip.

Table 3: CFD Model Parameters

Case	**Single Phase**	**Two Phase**
1	Standard Mesh	
2	Refined Mesh	
3		50,000 Tracks
4		100,000 Tracks
5		Spherical Drag (Shape Factor = 1.0) and Ideal Wall Collision (e_h=1.0, μ=0).
6		Ideal Wall Collision (e_h=1.0, μ=0).
7	Burner Internals	
8		Burner Internals
All cases are consistent with a base case (Standard Mesh, 50,000 Particle Tracks, model parameters as described) with deviations from this stated above.		

Table 4: CFD Cases

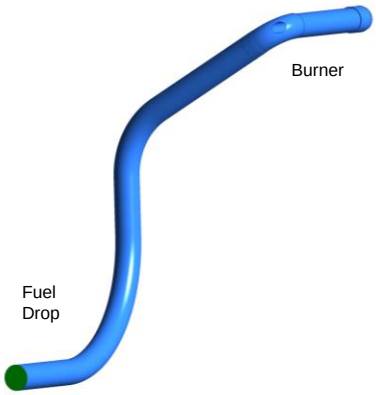

Figure 1: Burner and inlet pipe configuration.

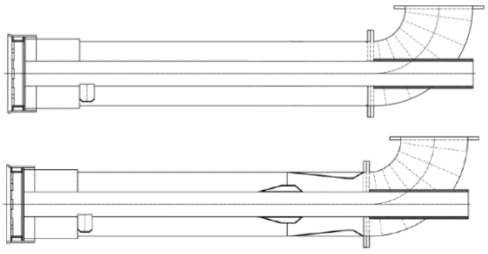

Figure 2: Burner geometry with no internals (top), with internals (bottom).

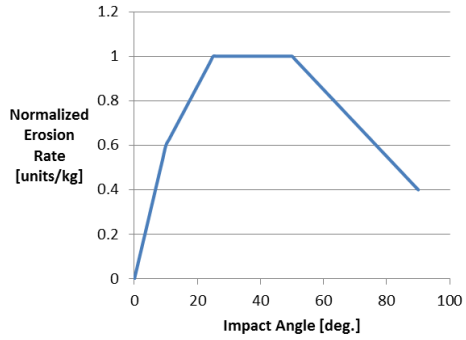

Figure 3: Normalised erosion rate curve for ductile materials and utilised in Equation 13. Based on erosion rate curves reported by Mills (2004) and Schade (2002).

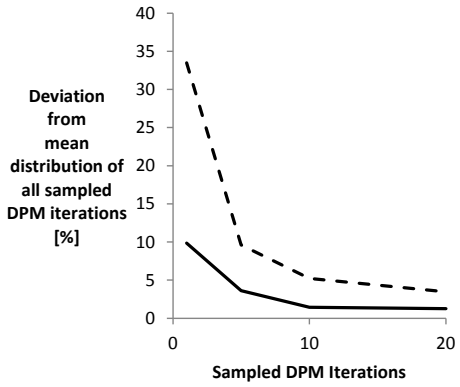

Figure 4: Due to cycling of the outlet concentration monitors the outlet distribution was averaged over 20 DPM iterations to reduce the variation to <5% between dpm iterations. ---- mean of all outlets, - - - max of all outlets.

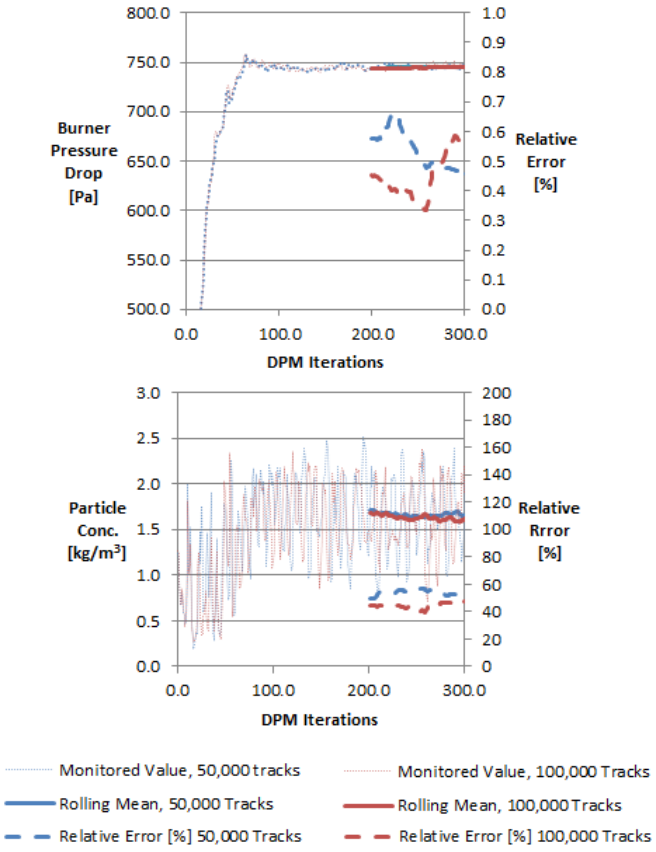

Figure 5: Demonstration of convergence for burner pressure drop and outlet concentration including particle track independence check.

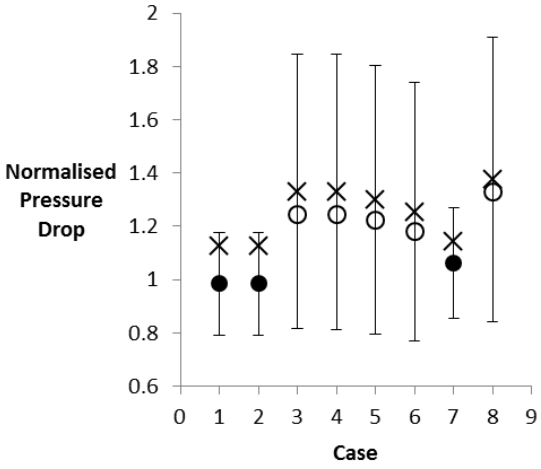

Figure 6: Normalised burner pressure drop against experimental result. Mesh independence, cases 1 and 2. Particle track independence, cases 3 and 4. Wall collision model parameter sensitivity, cases 5 and 6. Burner with internals, cases 7 and 8.
[●] single phase flow, pressure tapping locations
[o] two phase flow, pressure tapping locations
[x] average static pressure across burner inlet plane

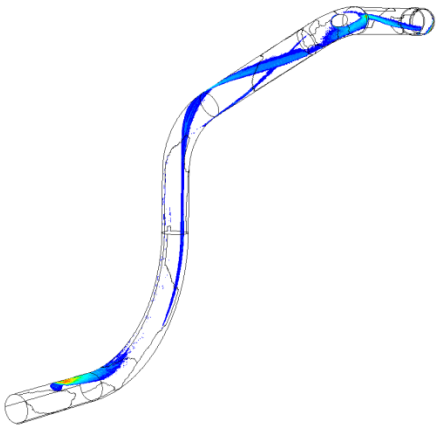

Figure 7: Location of the particle rope within the geometry. Iso-surface of discrete phase volume fraction clipped between 0.01-0.1m^3/m^3.

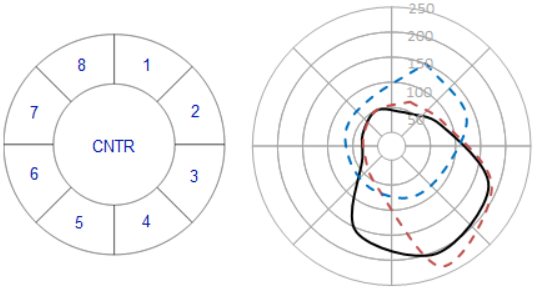

Figure 8: Normalized outlet distribution [%]. Experimental outlet configuration (left), CFD and experimental comparison (right).
[---] Experiment, CNTR 110%
[---] Case 3, CNTR 150%
[---] Case 5, CNTR 164%

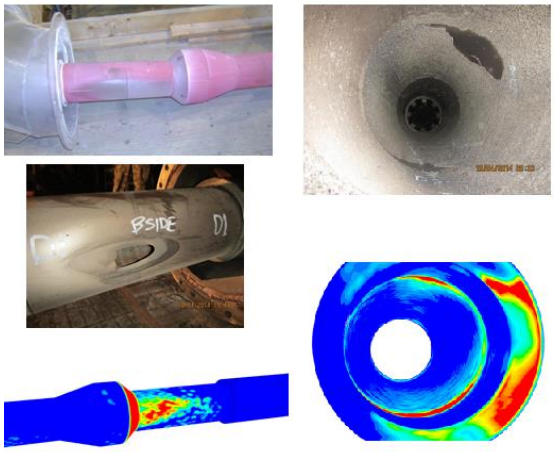

Figure 9: Comparison of erosion wear on inside (left) and outer wall (right) for the burner geometry with internals.

ACKNOWLEDGEMENTS

The author gratefully acknowledges the support of his Doosan colleagues, especially Graham Lewis and Jim Rogerson, and those at Nels Consulting Services Ltd. who obtained the experimental data. Dr. Donald Giddings and Prof. Henry Power at The University of Nottingham who supervised a lot of the CFD model development.

REFERENCES

BRITISH STANDARDS INSTITUTION (2005), "Measurement of fluid flow – Procedures for evaluation of uncertainties", BS ISO 5168:2005

DENIS, S. SINGH, S., INGHAM, D. (1980), "The steady flow due to rotating sphere at low and moderate Reynolds numbers" *Journal of Fluid Mechanics*, **101**, 257-279

GIDDINGS, D., AROUSSI, A., PICKERING, S.J., and MOZAFFARI, E., (2004), "A ¼ scale test facility for PF transport in power station pipelines", *Fuel*, **83**, 2195-2204.

HAIDER, A. and LEVENSPIEL, O. (1989), "Drag Coefficient and Terminal Velocity of Spherical and Nonspherical Particles", *Powder Technology*, **58**, 63-70.

LAÍN, S. and SOMMERFELD, M., (2008), "Euler/Lagrange computations of pneumatic conveying in a horizontal channel with different wall roughness", *Powder Technology*, **184**, 76-88.

LAÍN, S. and SOMMERFELD, M. (2013), "Characterisation of pneumatic conveying systems using the Euler/Lagrange approach", *Powder Technology*, **23,** 764-782

LI, J., and KWAUK, M., (1994), "*Particle Fluid Two-phase Flow: The Energy-Minimization Multi-Scale Method*", Metallurgical Industry Press, China, Beijing.

LOVE, A., GIDDINGS, D., POWER, H. (2015), "Gas-particle flow modelling: beyond the dilute limit", *The 7th World Congress on Particle Technology (WCPT7), Procedia Engineering*, **102,** 1426-1435

MILLS, D. (2004), "Pneumatic Conveying Design Guide", Second Edition, Elsevier Butterworth Heinemann.

OESTERLE, B. and JEAN, A. P. (1993), "Simulation of particle-to-particle interactions in gas-solid flows", *International Journal of Multiphase Flow*, **19**, 199-211

SCHADE, K., ERDMANN, H., HADRICH, T. SCHNEIDER, H. FRANK, T. and BERNET, K., (2002), "Experimental and numerical investigation of particle erosion caused by the pulverised fuel in channels and pipework of coal-fired power plant", *Powder Technology*, **125**, 242-250.

SCHNEIDERBAUER, S., PUTTINGER, S. and PIRKER, P. (2013), " Verification of sub-grid drag modification for dense gas-particle flows in bubbling fluidized debs", *The 14th International Conference on Fluidization – From Fundamentals to Products*, ECI Symposium Series.

SOMMERFELD, M. and HUBER, N., (1999), "Experimental analysis and modelling of particle-wall collisions", *International Journal of Multiphase Flow*, **25**, 1457-1489.

TSUJI, Y. and MORIKAWA, Y. (1982), "LDV measurements of an air-solid two phase flow in a horizontal pipe", *Journal of Fluid Mechanics*, **120,** 385-409